ISSN 1990-519X, Cell and Tissue Biology, 2021, Vol. 15, No. 1, pp. 90–97. © Pleiades Publishing, Ltd., 2021.
Russian Text © The Author(s), 2020, published in Tsitologiya, 2020, Vol. 62, No. 6, pp. 437–445.

Changes in the Fluorescence Characteristics of Quantum Dots Based on InP/ZnS during the Interaction with Cells

I. K. Litvinov[a, *], T. N. Belyaeva[a], E. A. Leontieva[a], A. O. Orlova[b], and E. S. Kornilova[a, c]

[a] *Institute of Cytology, Russian Academy of Sciences, St. Petersburg, 194064 Russia*
[b] *ITMO University, St. Petersburg, 197101 Russia*
[c] *Peter the Great St. Petersburg Polytechnic University, St. Petersburg, 195251 Russia*
**e-mail: lik314@mail.ru*

Received February 20, 2020; revised March 5, 2020; accepted March 10, 2020

Abstract—Semiconductor quantum dots (QDs), due to their unique spectral-luminescent properties, are attractive for visualizing biological objects in biological and medical research. The main methods for registering luminescent QDs in the cells are various types of scanning microscopy. It is important to note that during the use of QDs, they are delivered into different extracellular and intracellular environments, which can affect the surface integrity of QDs and, as a result, the photophysical characteristics of QDs. In this connection, changes in the characteristics of the luminescence signals of non-target QDs based on InP/ZnS, coated with polyethylene glycol with COOH-groups, were studied, which can reduce the risk of toxic effects in the process of biological and medical research. In this work, QDs-InP accumulated in endosomes of A549 cultured cells. Analysis of the photophysical properties of QDs showed that the average intensity of QDs in endosomes was lower than the intensity of clusters outside the cells, which can be explained by a lower concentration of QDs in intracellular clusters. However, the QDs luminescence lifetime in clusters, independent of concentration, was also 5–10 ns lower. Analysis of the QDs solution showed that a decrease in the quantum yield and QDs luminescence lifetimes is observed in solution with pH 4.0, but not 7.4–8.0. Also, the process of significant formation of QDs aggregates in such solutions was not revealed. In this connection, changes in the photophysical properties of QDs interacting with cells, can be associated with the entry into endosomes with a low pH level. Thus, the analysis of the luminescence lifetimes of QDs allows to obtain additional information about their state in comparison with the determination of the fluorescence intensity. Our results are important for an adequate interpretation of data concerning both the efficiency of QDs uptake and analysis of the properties of intracellular compartments in which QDs accumulate.

Keywords: InP/ZnS quantum dots, luminescence intensity, FLIM, luminescence lifetime, endosomes, pH, A549 cells

DOI: 10.1134/S1990519X21010065

The application of semiconductor quantum dots (QDs) for biological objects visualization is a relatively new area of research. The uniqueness of QDs is determined by their properties such as a wide absorption spectrum, narrow luminescence spectra, which depend on the size of the semiconductor core of a QDs, and a large Stokes shift. The high photostability of QDs, which makes it possible to carry out relatively long lifetime observations, is also attractive.

QDs can be obtained from compounds of elements II–VI, III–V, or IV–VI groups of the periodic system of chemical elements. For biological research, core-shell QDs are most often used. QDs nuclei usually consist of CdSe, CdTe, InP, etc. Usually, ZnS is used as a shell. The sizes of such nanoparticles, which determine the fluorescence wavelength, are in the range of 2–9 nm. Since the synthesis of QDs is mainly carried out in a hydrophobic medium, to ensure biocompatibility, QDs are coated with a layer of amphiphilic compound, which is most often used polyethylene glycol (PEG). It effectively reduces nonspecific binding to cells and is inert to the immune system. In addition, by using various functional groups of the modified PEG, QDs can be conjugated to biomolecules of interest, such as antibodies or ligands to surface receptors. This turns non-targeted QDs into targeted ones and makes it possible to visualize various biological processes in certain cells, which is important for basic research (Wegner et al., 2015). In addition, since the functionalization of QDs using PEG carrying multiple active groups significantly increases the particle size (up to 15–30 nm), and accordingly its

Abbreviations: QDs-InP—quantum dots based on InP/ZnS coated with polyethylene glycol with COOH-groups; PEG—polyethylene glycol.

surface area, such QDs can be used as multifunctional platforms for medical diagnostics, i.e. QDs having a molecular address and QDs modified depending on the task with a drug or, for example, a photosensitizer.

The most commonly used are QDs based on CdSe/ZnS. This is due to the fact that, firstly, the method of chemical colloidal organometallic synthesis of such QDs is well developed and gives a stable result, and, secondly, their luminescence spectrum covers almost the entire visible spectrum. However, cadmium due to the binding of carboxyl, amine and sulfhydryl groups of protein molecules can inhibit the activity of many enzyme systems. Therefore, despite the fact that QDs-CdSe are coated with a ZnS layer, they are afraid to use them for medical purposes.

Indeed, theoretically, there is a risk of cadmium ion leakage during prolonged exposure of the QDs in an active biological medium as a result of damage to the shell due to the high level of reactive oxygen species (Kirchner et al., 2005; Smith et al., 2008). Nevertheless, it should be borne in mind that the size of functionalized non-targeted QDs-PEGs makes it possible for them to enter cells only through different types of endocytosis, as a result of which QDs are isolated from the cytoplasm in membrane vesicles - endosomes. The main factor of external influence in this case is a decrease in the pH level in endosomes as they pass through the successive stages of the endocytotic pathway, from 7.4–7.0 in the early stages of endocytosis to 4.0–4.5 in lysosomes, where non-targeted QDs enter after several hours and where they can persist for several days. Indeed, such effects have been demonstrated in a number of works (Aldana et al., 2001, 2005; Derfus et al., 2004; Bentzen at al., 2005; Uyeda et al., 2005). Nevertheless, the solution to the problem of taking these effects into account during QDs cellular uptake is still under development (Martynenko et al., 2016).

Obviously, any risks should be minimized. One way to solve this problem is to use "cadmium free" QDs, for example, based on indium phosphide (InP) (Young et al., 2012), however, various aspects of their interaction with cells are still not well understood.

It should be noted that QD is a nanocrystal consisting of an inorganic core and an organic shell, i.e. an ensemble of particles capable of exhibiting a rather complex behavior in case of integrity violation or when interacting with surrounding molecules (ions). In semiconductor QDs, the absorption of light leads to the excitation of electrons and their transition from the valence band to the conduction band, leaving behind the holes—quasiparticles that are carriers of a positive charge. The charge carriers in semiconductor QDs—an electron and a hole—function as a single quantum-mechanical system: an electron-hole pair (e-h pair). In the literature, such pair is called an exciton.

During the transition of an electron back to its ground state—the valence band, radiation occurs in the form of a quantum of light (the exciton recombines). An excited QD can consume photoexcitation energy as a result of radiative or non-radiative deactivation of an excited state (Lakowicz et al., 2007). The ratio of the rates of radiative and nonradiative transitions is determined by such parameters as the quantum yield and luminescence lifetime. The larger the fraction of radiative recombinations with respect to nonradiative ones, the higher the fluorescence intensity, quantum yield (φ), and luminescence lifetime ($\langle\tau\rangle$) (also called the decay time) of QDs.

The fluorescence intensity (I), therefore, is positively associated with these parameters, however, practically assessing the intensity does not give the researcher information about the state of QDs in the endosomes for the following reasons. First, in contrast to the quantum yield and QDs luminescence lifetime, the luminescence intensity depends on the concentration of fluorescence sources in the analyzed objects (i.e., on the concentration of the QDs itself). Secondly, the luminescent signals of cells that uptake fluorophores are recorded by fluorescence confocal microscopy during prolonged irradiation of the entire field, and the differences in the photophysical parameters of individual elements of QDs ensembles are substantially eliminated. Thus, when analyzing the luminescence signal obtained using a confocal microscope, differences in the intensity of QDs luminescence outside and in the cells do not allow us to unambiguously conclude that the reasons for these differences are associated with different concentrations of QDs, or with QDs luminescence quantum yield, or one and the other at the same time. Therefore, it is necessary to correctly investigate the state of QD in cells, analyzing the kinetics of their luminescence decay.

In the experimental determination of the averaged $\langle\tau\rangle$ value using a laser scanning microscope, excitation is carried out by a femtosecond laser pulse followed by registration of single photons in the selected channel of wavelengths for a certain time. Further, when processing data using instrumentation software, it is possible to determine $\langle\tau\rangle$ the area of interest to us. As noted above, damage to the surface of the QDs or their aggregation affects the determined value, which makes it possible to obtain information about the state of QDs in the studied objects.

In this work, we studied the possibility of QDs cellular uptake by A549 cells with using QDs based on InP/ZnS coated with PEG containing COOH groups (QDs-InP), compared the average luminescence lifetime of QDs ($\langle\tau\rangle$), QDs clusters outside and inside the cells, and simulated the effect of different pH values of the solution on the photophysical characteristics of QDs.

MATERIALS AND METHODS

Materials. InP/ZnS based QDs with a PEG shell with COOH groups (QDs-InP) with a luminescence maximum at 640 nm were used (Mesolight, China).

The cultivation of cells. A549 human lung adenocarcinoma cells from the Russian collection of cell cultures of the Institute of Cytology RAS (St. Petersburg) were cultured in 25 cm^2 vials or 96-well plates (Nunc, USA) in DMEM medium (Biolot, Russia) containing 20 mM glutamine, 10% fetal bovine serum, 0.1% gentamicin, in the atmosphere of 5% CO_2 at 37°C. Cells for experiments were seeded on coverslips in Petri dishes (Nunc, USA) and experiments were performed after 48 h when the cells reached a 60–70% monolayer. QDs at the required concentration were added to the cell culture medium for 24 hours. Then, the cells were fixed with 4% paraformaldehyde for 15 min.

Confocal microscopy. The studies were performed using an Olympus FV3000 laser scanning confocal microscope (Japan). Used oil immersion lens 40/1.42×. The fluorescence of QDs was excited by a laser with a wavelength of 405 nm and was recorded in the region of 600–680 nm. Images were taken in a spectral channel corresponding to the fluorescence detection region of specific QDs and using the method of differential interference contrast in transmitted light. Single sections or serial Z-series with a step of 0.5 μm were recorded (10–20 consecutive optical sections).

Spectral and luminescent properties of QDs-InP. The method of stationary optical spectroscopy was used. The quantum yield of QDs luminescence (φ) was calculated on the basis of data obtained on a UV-3600 spectrophotometer (Shimadzu, Japan) and a Cary Eclipse spectrofluorimeter (Aligent, United States).

Registration of the luminescence decay kinetics of QDs-InP. A MicroTime 100 laser scanning luminescent microscope (PicoQuant, Germany) operating in the single-photon counting mode was used. In the present work, luminescence decays of nanostructures (QDs luminescence lifetimes, τ) were recorded using interference optical filters characterized by transmission bands with a width of 10 nm at a level of 50% of the transmission maximum at 600, 640, and 680 nm.

QDs-InP τ was studied in phosphate-buffered saline (PBS) at pH 4.0, 7.4 or 8.0, as well as on cells of the A549 line. The desired pH of the PBS solution was adjusted by adding HCl or NaOH.

Statistical data processing. All results were obtained from at least three independent experiments. When examined with a confocal microscope, at least 4 visual fields (about 15–20 cells) were examined for each case. Images for presentation were processed using Adobe Photoshop 5.0. The obtained images were analyzed using the ImageJ program (National Institute of Health, USA). Statistical data processing was performed using Microsoft Office Excel 2007 (Microsoft Corporation, USA). The approximation of the decay curves of QDs luminescence was performed using the Origin Pro 8.5 software; Charts were built using Microsoft Office Excel 2007.

RESULTS AND DISCUSSION

Interaction of A549 cells with QDs-InP. The main methods for registering luminescent QDs in cells are various types of scanning microscopy. We used a confocal microscope. Figure 1a shows a typical confocal image of A549 cells fixed after incubation with QDs-InP for 24 hours, combined with the image in differential interference contrast, which allows to see both the contours of the cells and the localization of the fluorescent signal in intracellular vesicular structures (endosomes) of different sizes (examples are indicated by thin arrows). The picture of the intracellular distribution of QDs-InP basically coincides with that which we observed earlier for non-targeted QDs based on CdSe/ZnS with the same organic shell (Litvinov et al., 2018) and suggests the possibility of using QDs-InP as a biological label.

Analysis of the Z-series of images of these cells also made it possible to identify clusters of QDs localized on the surface of the cells (an example is indicated by the arrowhead). Thus, a small part of the studied QDs non-specifically binds to the cell surface during a long incubation. (We did not analyze such clusters in the present work.) At the same time, some of the QDs remain on the substrate, and judging by the size, they are not single QDs (thick arrows). To simplify the further discussion, we will call such ensembles of luminescent objects both inside cells (i.e., in endolysosomes) and outside the cells on a substrate, "clusters". Visually, the clusters both outside and inside the cells vary significantly in size, but the difference in the luminescence intensity of QDs is not so obvious. However, the assessment on the image (Fig. 1b) of the average intensity of one pixel of the cluster outside the cells (12 selected objects) and inside them (76 selected objects) shows that this value is about a third lower in intracellular clusters than in extracellular ones, while the average the intensity of the clusters themselves is about 4 times less.

The interpretation of this data is extremely difficult. The result, obviously, can be affected by the unequal number of analyzed clusters outside and inside the cell, as well as the more significant contribution of small objects to the average intensity of intracellular clusters. However, it is more likely that the reason is that QDs are extinguished in the process of entering the endosomes. On the other hand, it is possible that part of the QDs inside the cells either does not undergo a concentration process in the lysosomes or has already left the cell as a result of the process of

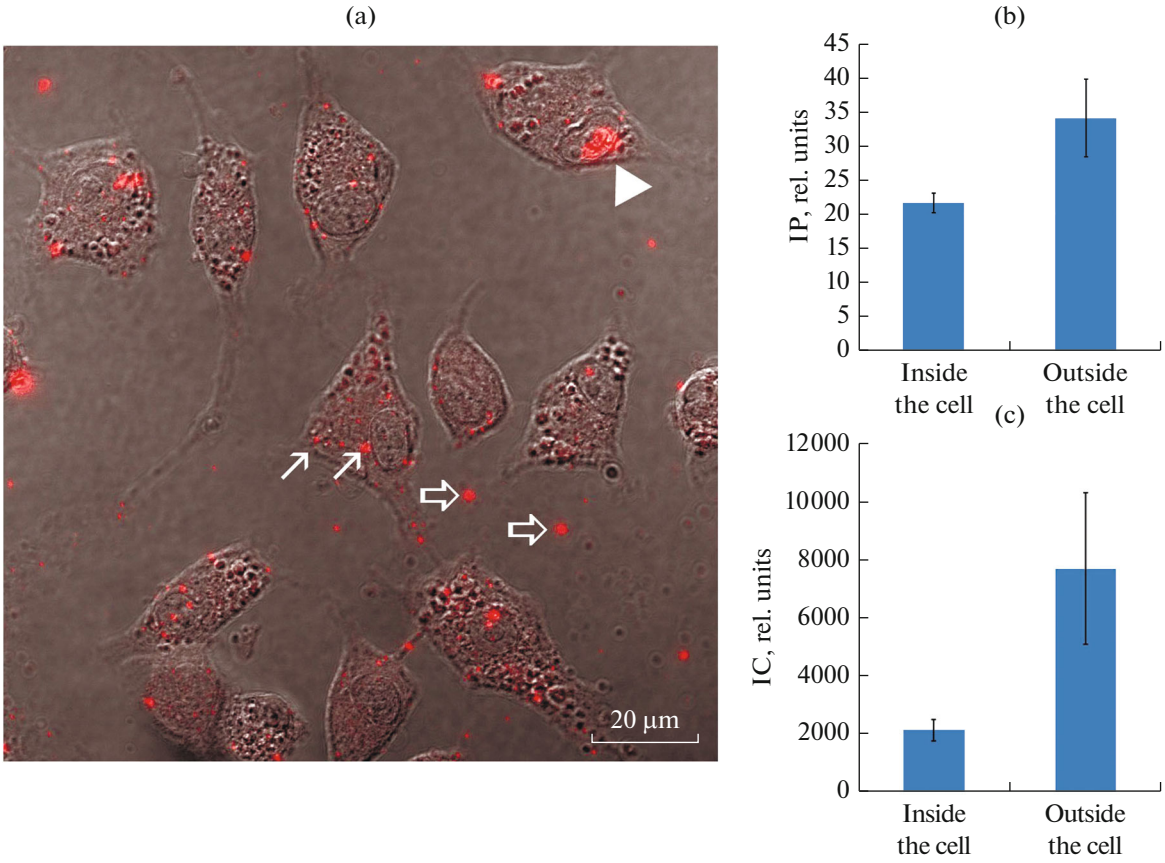

Fig. 1. Visualization of InP/ZnS-based quantum dots coated with PEG having COOH groups (QDs-InP, 20 nM) in A549 cells fixed after 24 hours of cultivation in the presence of QDs-InP. (a) image of cells and QDs obtained using a laser scanning microscope Olympus FV3000 (Japan); superposition of the QDs luminescence channel (red) and differential-contrast image of cells (gray) is presented; thin arrows show particular examples of QDs clusters inside the cells, thick arrows show QDs clusters outside the cells, the head of the arrow indicates the accumulation of QDs on the cell surface. (b, c) Distribution of the average pixel luminescence intensity in a cluster (IP, b) and the average cluster intensity (IC, c) in image a. Average intensities were calculated for 76 clusters inside the cells and 12 clusters outside the cells.

exocytosis of endolysosomes. More definite conclusions based on such an analysis cannot be drawn.

During the analysis of the decay kinetics of luminescent objects using a PicoQuant microscope designed to record fluorescence lifetime by FLIM method (Fluorescence-Lifetime Imaging Microscopy), we can obtain data that do not depend on the concentration of QDs in the clusters and which indicate whether the properties of QDs are different inside and outside the cells.

As mentioned above, a QD excited by a laser pulse can consume photoexcitation energy as a result of both radiative and nonradiative deactivation of the excited state (Lakowicz et al., 2007). If we denote the radiative transition rate constant k_r, and the total constant of all other processes leading to nonradiative deactivation of the excited state is k_{nr}, then the luminescence quantum yield (φ) can be calculated by the equation:

$$\varphi = \frac{k_r}{k_r + k_{nr}}, \quad (1)$$

and the luminescence lifetime τ by:

$$\tau = \frac{1}{k_r + k_{nr}}. \quad (2)$$

Obviously, the emergence of new channels of nonradiative deactivation of the excited state of quantum dots, the rate constant of which is comparable to or greater than kr, will lead to a decrease in φ and τ due to the mechanisms of quenching of luminescence for the following reasons: nonradiative transfer of photoexcitation energy (Förster resonance energy transfer, FRET) from quantum dots to external molecules or neighboring QDs; charge carrier transfer (a QDs electron in an excited state can interact with electron-acceptor molecule, or an electron-donor molecule can give an electron to QD). This situation of quenching of the luminescence of QDs can occur when the surface of QDs is damaged, when additional molecules are included in the ensemble, and when aggregates are formed.

QDs τ is determined from the kinetics of multiexponential decay (Schlegel et al., 2002). In theoretical models, the deviation from the monoexponential decay of the QD luminescence is associated with the disordering of the crystal lattice of the QD core and an increase in the number of surface defect states leading to the multiexponential dependence of the luminescence attenuation described by the Kohlrausch-Williams-Watts function:

$$I(t) = \sum_n \left(A_n e^{\frac{t}{\tau_n}} \right), \quad (3)$$

where A_n are the components of the amplitude and τ_n are the components of the luminescence lifetime of nanostructures In most cases, the three-exponential dependence is closest to the experimental data, where n is 1, 2, and 3. The average luminescence lifetime of QDs ($\langle\tau\rangle$) is determined by the equation:

$$\langle\tau\rangle = \frac{\sum_n A_n \tau_n^2}{\sum_n A_n \tau_n}. \quad (4)$$

During the analysis PicoQuant microscope scans the area of interest, usually with a resolution of 512 × 512 pixels. The luminescence decay curve is built up over the scanned area with the instrument software, the approximation of which determines the distribution of the luminescence decay times over the entire sample with the formation of a τ histogram. According to this histogram, each pixel of the scanning section corresponds to its own value of τ, determined by the color scale of values on the τ histogram. Thus, in accordance with the data of the histogram τ, a color FLIM image of the scan area is formed.

In Fig. 2, in the form of a FLIM visualization, scanning data of a glass section with A549 cells recorded 24 hours after incubation with QDs-InP at a concentration of 20 nM is presented.

The scan data presented in Fig. 2 made it possible to separately identify the QDs clusters of interest to us (inside and outside the cells) from FLIM visualization, to calculate their $\langle\tau\rangle$. For the selected QDs clusters, individual luminescence decay curves were derived (Figs. 3a, 3b), the approximation of which calculated the values of $\langle\tau\rangle$. From the data of table 1, it follows that for QDs, the values of $\langle\tau\rangle$ of these types of clusters differ by approximately 5–10 ns. Thus, we can

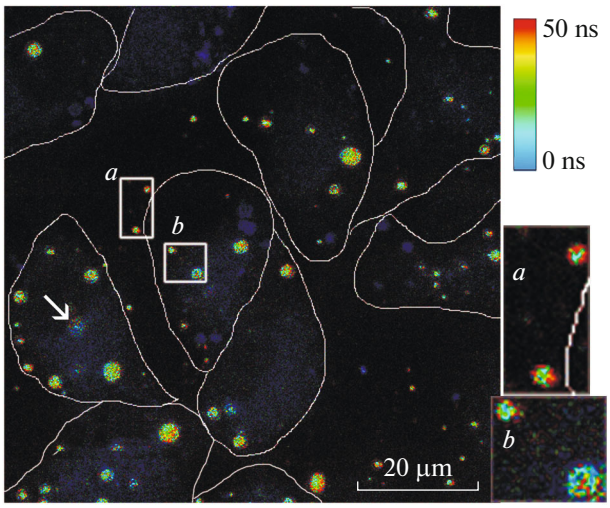

Fig. 2. FLIM (fluorescence lifetime imaging) – imaging of QDs-InP (20 nM) in A549 cells fixed after 24 h of cultivation in the presence of QDs obtained using a laser scanning microscope (MicroTime 100; PicoQuant, Germany). Cells are outlined. At the top right is a color scale that reflects the luminescence lifetimes on FLIM imaging. (a, b) 3 times enlarged areas with QDs, respectively indicated on the main image. The arrow indicates an example of a large cluster inside the cell with a very short lifetime.

conclude that during the QDs cellular uptake, the photophysical characteristics of QDs change.

Visual analysis of the clusters $\langle\tau\rangle$ (Fig. 2) allows to make several more interesting observations. Thus, the general nature of the color of the clusters suggests that, firstly, the spread in lifetimes in both the group of extracellular and in the group of intracellular clusters is much larger than the spread of intensities, and, secondly, within a single cluster, there may be areas with different lifetimes. Interestingly, extracellular clusters are characterized by the presence of long-lived (red) regions mainly along the outer edge of the cluster and shorter luminescence lifetimes in the center of the cluster (see Fig. 2a). For intracellular clusters, the distribution is more complicated: for example, small peripheral clusters have more regions with a long-lived signal similar to an extracellular one, while larger ones mostly show shorter luminescence decay times, while remaining non-uniform (Fig. 2b).

In addition, rather large clusters with very short lifetimes are located inside the cells (Fig. 2, indicated by an arrow). It is reasonable to assume that extracel-

Table 1. Approximation of the luminescence decay curves in accordance with the three-exponential model

Clusters	A_1, rel.un.	A_2, rel.un.	A_3, rel.un.	τ_1, ns	τ_2, ns	τ_3, ns	$\langle\tau\rangle$, ns
Inside the cells	0.59 ± 0.03	0.33 ± 0.01	0.08 ± 0.03	35.0 ± 1.6	6.0 ± 0.4	0.6 ± 0.4	32.0 ± 1.2
Outside the cells	0.42 ± 0.08	0.31 ± 0.04	0.27 ± 0.09	46.0 ± 3.3	8.3 ± 1.5	0.2 ± 0.1	42.0 ±7.6

The approximation was carried out according to equation (3). The values of the amplitude components (A) and the corresponding luminescence lifetimes (τ) are given.

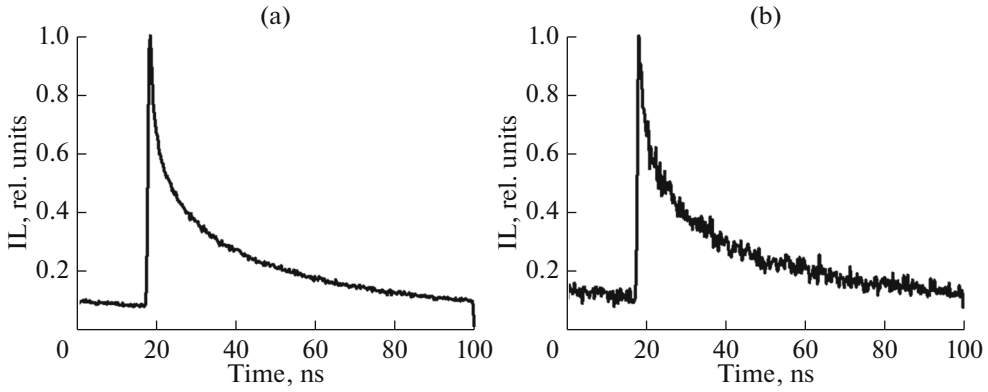

Fig. 3. Luminescence decay curves of QDs-InP (20 nM) in A549 cells, fixed after 24 h of cultivation in the presence of QDs, obtained from the image analysis in Fig. 2. For QDs clusters inside and outside the cells, separate luminescence decay curves were obtained. a, b – Averaged damping curves of the luminescence intensity (IL) of QDs clusters inside (a) and outside (b) of the cells. IL is normalized to the maximum value of the luminescence signal.

lular clusters are more aggregated in the center and less aggregated at the periphery of the cluster, possibly formed during storage of the stock solution of QDs or sticking to the substrate. Clusters of QDs localized in cells could arise by internalizing QDs in the early endosomes and then quench as they are moved through the endocytotic pathway, the main characteristic of which is a decrease in intraendosomal pH from 7.4 to 4.0–4.5 in lysosomes. Also, the possibility of their aggregation with a change in pH is not excluded. To test these assumptions on in vitro model systems, we determined φ and ⟨τ⟩ QDs, which allow one to evaluate the effect of acidification on QD properties and their degree of aggregation.

To study the effect of the pH of the solution on the photophysical characteristics of QDs, we used a solution of QDs-InP in PBS at a concentration of 80 nM with different pH values. The values of φ were analyzed using a spectrophotometer and a spectrofluorimeter. The quantum yield of luminescence of nanostructures was determined using the comparison method, in which a sample was used (as a reference) with a known value of the quantum yield of luminescence (rhodamine 6G, φ = 95%). Figure 4 shows the values of φ for QDs depending on the pH of the PBS solution and depending on the incubation time in it.

The measurement results in Fig. 4 shows that the effects of alkali (pH 8.0) and normal state (pH 7.4) are negligible: the values of φ remain in the range of 9–10% throughout the entire experiment, whereas in an acidic PBS solution (pH 4.0), a sharp decrease in the luminescence quantum yield of QDs from 10 to 7%, however, further incubation in an acidic medium practically does not affect this value, which remains within the margin of error.

The effect of pH can be explained by both quenching of fluorescence and stimulation of aggregation, in which ⟨τ⟩ also decreases. The following approach was used to assess the degree of aggregation. It is believed that this process is accompanied by the shift of the maximum in the luminescence spectrum to the right, in the region of longer waves. This is because the actual size distribution of QDs has a certain scatter and, when aggregated, QDs of different sizes are included in the ensemble, thereby increasing the probability of FRET from smaller QDs to larger QDs, since the probability of nonradiative exciton recombination sharply increases in aggregates. At the same time, the luminescence of small QDs-donors in the aggregates is quenched, and large QDs-acceptors remain unquenched.

We determined the QDs luminescence lifetimes at three points corresponding to the position of the luminescence maximum (640 nm), to the left and right of it at half the height of the luminescence band (600 and

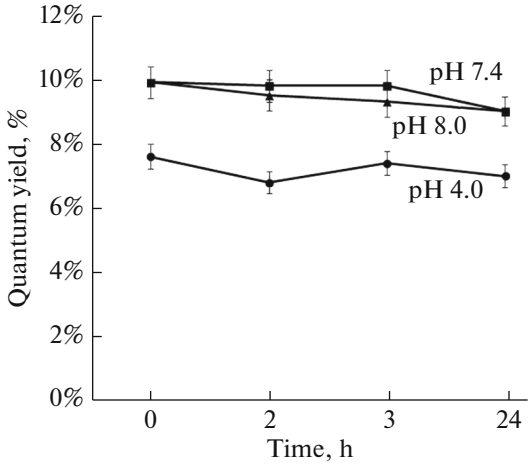

Fig. 4. Quantum yield of QDs-InP luminescence in PBS solutions. The measurements were carried out at pH 4.0, 7.4, and 8.0 immediately after the introduction of QDs into the solution (0 h) and after 2, 3, and 24 h of incubation in the solution.

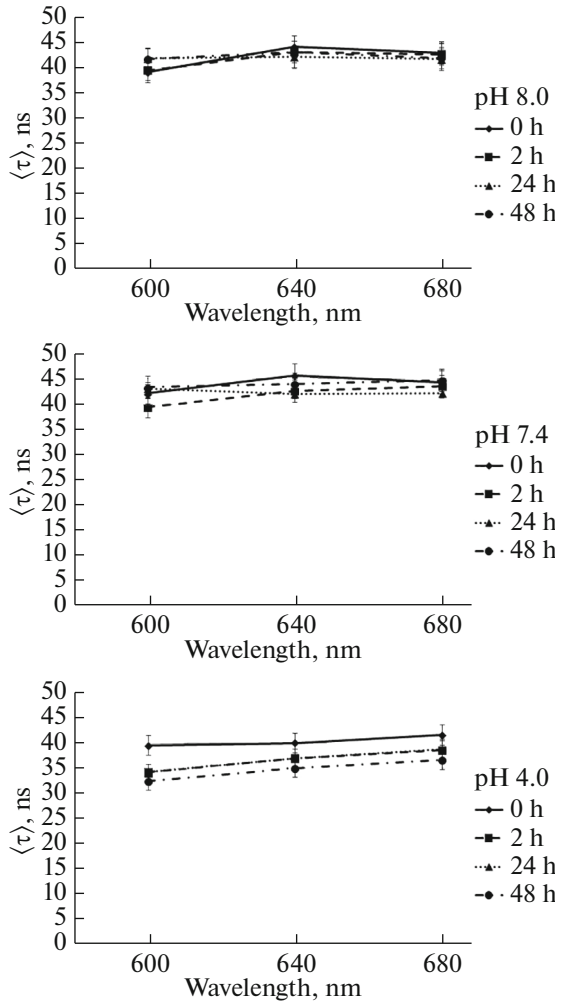

Fig. 5. The average lifetime of the luminescence of QDs-InP (⟨τ⟩) in PBS solutions. The measurements were carried out at pH values of 8.0, 7.4, and 4.0 immediately after the injection of QDs into the solution (0 h) and after 2, 3, and 24 h of incubation in the solution. Optical interference filters were used, characterized by transmission bands with a width of 10 nm at a level of 50% of the maximum transmission at a wavelength of 600, 640, and 680 nm.

680 nm). To obtain the data, a pulsed laser scanning microscope with interference filters transparent at these wavelengths was used. As a result of the analysis of the kinetics of the decay of the QD luminescence at these wavelengths, the corresponding QDs luminescence lifetimes were obtained. The data are presented in Fig. 5.

From the QDs luminescence decay kinetics at a wavelength corresponding to its maximum luminescence (640 nm), it follows that upon incubation of QDs for 0-48 h in normal (pH 7.0) and alkaline (pH 8.0) PBS solution, the lifetime decreases from 45 to 42 ns, and in an acidic PBS solution (pH 4.0)—from 40 to 35 ns. However, these differences were within the measurement error. Measurement of the same parameter of QDs (τ) at 600 and 680 nm did not show significant changes in time compared to the zero point. However, at pH 4.0, an insignificant increase in τ was observed from the shorter wavelength to the larger after 2 h of incubation, but in the future it did not increase anymore. This may indicate that the fraction of aggregates does not change during incubation of QDs at high pH values; however, at pH 4.0 typical of lysosomes, there is a slight tendency to increase the share of QDs aggregates, which follows from the largest value of τ in the case of measurements at a wavelength of 680 nm

Since changes in the photophysical characteristics of QDs directly depend on the integrity of the QDs structure and the influence of molecules of the external environment, it can be assumed that for QDs-InP, the influence of H^+ ions leads to the appearance of defect states on the surface of the QDs shell and the formation of trap states leading to disruption of the carrier recombination processes, and, as a result, both the quantum yield of luminescence and the luminescence lifetime of QDs decrease.⟨⟩

In the present work, it was shown that QDs-InP are detected in cells inside compartments in the form of clusters available for analysis of accumulation and determination of photophysical characteristics, in particular, estimates of the decay times of QDs luminescence. Analysis of the luminescence decay time on a fixed cell preparation and in vitro approaches have shown that QDs luminescence is quenched in the endosomes of cells, therefore, the assessment of their intracellular accumulation by the fluorescence intensity is underestimated. It is essential to emphasize that we analyzed the lifetimes for fixed cells. This was done due to the fact that scanning an area containing a sufficient number of cells for statistical analysis takes too much time (tens of minutes). During this time, the state and distribution of QDs can change during endocytotic processes and, in addition, intravital preparations exist in nonphysiological conditions.

Earlier, we showed that fixation substantially eliminates the spread in the values of lifetimes between individual endosomes (Litvinov et al., 2018), so that the development of a technique for lifetime recording of luminescence decay in living cells, which allows us to estimate ⟨τ⟩, can give a more significant difference and, accordingly, a more significant amendment. Moreover, the role of endosome acidification in quenching the luminescence of QDs in endolysosomes seems to be more significant than their aggregation.

Recently, methods for processing and analyzing fluorescence images of cells are becoming more widespread, in particular, for assessing the quantitative parameters of the dynamics of processes such as endocytosis (Collinet et al., 2010; Tonti et al., 2015). Therefore, the understanding of possible data distortions based only on the intensity of the fluorophore-labeled

protein without taking into account the nature of the fluorophore and its response to the microenvironment becomes an extremely urgent task.

To summarize this work, we can state that non-targeted InP-based QDs behave similarly to the same cadmium-based QDs, demonstrating accumulation in cells and sensitivity to acidic pH. Despite the fact that the photophysical characteristics of QDs-InP may vary depending on the composition of the core and the manufacturer, the main trends in behavior change remain. It should be emphasized the importance of the demonstrated effects on changes in the properties of QDs for an adequate interpretation of data concerning both the efficiency of absorption of QDs and intracellular localization of QDs. It was shown that QDs-InP can be used in small concentrations for labeling cells in general or intracellular targets of interest, which reduces the risks of possible toxic effects.

FUNDING

This work was financially supported by the Basic Research Program of the Presidium of the Russian Academy of Sciences no. 13 "Fundamentals of High Technologies and the Use of Features of Nanostructures in Nature Sciences" (project no. 3.1.2), the Russian Foundation for Basic Research (project no. 18-34-00382) and the Ministry of Science and higher education of the Russian Federation (state assignment no. 2019-1080).

COMPLIANCE WITH ETHICAL STANDARDS

The authors declare that they have no conflict of interest. This article does not contain any studies involving animals or human participants performed by any of the authors.

REFERENCES

Aldana, J., Lavelle, N., Wang, Y.J., and Peng, X.G., Size-dependent dissociation pH of thiolate ligands from cadmium chalcogenide nanocrystals, *J. Am. Chem. Soc.*, 2005, vol. 127, p. 2496.

Aldana, J., Wang, Y.A., and Peng, X., Photochemical instability of CdSe nanocrystals coated by hydrophilic thiols, *J. Am. Chem. Soc.*, 2001, vol. 123, p. 8844.

Bentzen, E.L., Tomlinson, I.D., Mason, J., Gresch, P., Warnement, M.R., Wright, D., Sanders-Bush, E., Blakely, R., and Rosenthal, S.J., Surface modification to reduce nonspecific binding of quantum dots in live cell assays, *Bioconjugate Chem.*, 2005, vol. 16, p. 1488.

Collinet, C., Stoter, M., Bradshaw, C.R., Samusik, N., Rink, J.C., Kenski, D., Habermann, B., Buchholz, F., Henschel, R., Mueller, M.S., Nagel, W.E., Fava, E., Kalaidzidis, Y., and Zerial, M., Systems survey of endocytosis by multiparametric image analysis, *Nature*, 2010, vol. 464, p. 243.

Derfus, A.M., Chan, W.C.W., and Bhatia, S.N., Probing the cytotoxicity of semiconductor quantum dots, *Nano Lett.*, 2004, vol. 4, p. 11.

Kirchner, C., Liedl, T., Kudera, S., Pellegrino, T., Muñoz, Javier, A., Gaub, H.E., Stölzle, S., Fertig, N., and Parak, W.J., Cytotoxicity of colloidal CdSe and CdSe/ZnS nanoparticles, *Nano Lett.*, 2005, vol. 5, p. 331.

Lakowicz, J.R., *Principles of Fluorescence Spectroscopy*, New York: Springer Science and Business Media, 2007.

Litvinov, I.K., Belyaeva, T.N., Salova, A.V., Aksenov, N.D., Leontieva, E.A., Orlova, A.O., and Kornilova, E.S., Quantum dots based on indium phosphide (InP): the effect of chemical modification of the organic shell on interaction with cultured cells of various origins, *Cell Tissue Biol.*, 2018a, vol. 12, p. 135.

Litvinov, I.K., Belyaeva, T.N., Bazhenova, A.S., Leontieva, E.A., Orlova, A.O., and Kornilova, E.S., QDs-cysteine luminescence kinetics: comparative analysis on live and fixed cells, in *Int. Conf. Laser Optics (ICLO), IEEE Proc.*, 2018b, p. 574.

Martynenko, I.V., Kuznetsova, V.A., Litvinov, I.K., Orlova, A.O., Maslov, V.G., Fedorov, A.V., Dubavik, A., Purcell-Milton, F., Gun'ko, Y.K., and Baranov, A.V., Enantioselective cellular uptake of chiral semiconductor nanocrystals, *Nanotechnology*, 2016, vol. 27, no. 7, p. 075102.

Schlegel, G., Bohnenberger, J., Potapova, I., and Mews, A., Fluorescence decay time of single semiconductor nanocrystals, *Phys. Rev. Lett.*, 2002, vol. 88. https://doi.org/10.1103/PhysRevLett.88.137401

Smith, A.M., Duan, H., Mohs, A.M., and Nie, S., Bioconjugated quantum dots for in vivo molecular and cellular imaging, *Adv. Drug Deliv. Rev.*, 2008, vol. 60, p. 1226.

Tonti, S., Di Cataldo, S., Bottino, A., and Ficarra, E., An automated approach to the segmentation of Hep-2 cells for the indirect immunofluorescence ANA test, *Comput. Med. Imaging Graph.*, 2015, vol. 40, p. 62.

Uyeda, H.T., Medintz, I.L., Jaiswal, J.K., Simon, S.M., and Mattoussi, H., Synthesis of compact multidentate ligands to prepare stable hydrophilic quantum dot fluorophores, *Am. Chem. Soc.*, 2005, vol. 127, p. 3870.

Wegner, K.D. and Hildebrandt, N., Quantum dots: bright and versatile in vitro and in vivo fluorescence imaging biosensors, *Chem. Soc. Rev.*, 2015, vol. 44, no. 14, p. 4792.

Young, K.T., Wang, Y., Roy, I., Rui, H., Swihart, M.T., Law, W.C., Kwak, S.K., Ye, L., Liu, J., Mahajan, S.D., and Reynolds, J.L., Preparation of quantum dot/drug nanoparticles formulations for traceable targeted delivery and therapy, *Theranostics*, 2012, vol. 2, p. 681.